NIH Public Access
Author Manuscript
Biochem Biophys Res Commun. Author manuscript; available in PMC 2010 December 25.

Published in final edited form as:
Biochem Biophys Res Commun. 2009 December 25; 390(4): 1177–1181. doi:10.1016/j.bbrc.2009.10.112.

Probing mechanisms for enzymatic activity enhancement of organophosphorus hydrolase in functionalized mesoporous silica

Baowei Chen, **Chenghong Lei***, **Yongsoon Shin**, and **Jun Liu**
Pacific Northwest National Laboratory, Richland, WA 99352, USA

Abstract

We have previously reported that organophosphorus hydrolase (OPH) can be spontaneously entrapped in functionalized mesoporous silica (FMS) with HOOC-as the functional groups and the entrapped OPH in HOOC-FMS showed enhanced enzyme specific activity. This work is to study the mechanisms that why OPH entrapped in FMS displayed the enhanced activity in views of OPH-FMS interactions using spectroscopic methods. The circular dichroism (CD) spectra show that, comparing to the secondary structure of OPH free in solution, OPH in HOOC-FMS displayed increased α-helix/β-strand transition of OPH with increased OPH loading density. The fluorescence emission spectra of Trp residues were used to assess the tertiary structural changes of the enzyme. There was a 42% increase in fluorescence. This is in agreement with the fact that the fluorescence intensity of OPH was increased accompanying with the increased OPH activity when decreasing urea concentrations in solution. The steady-state anisotropy was increased after OPH entrapping in HOOC-FMS comparing to the free OPH in solution, indicating that protein mobility was reduced upon entrapment. The solvent accessibility of Trp residues of OPH was probed by using acrylamide as a collisional quencher. Trp residues of OPH-FMS had less solvent exposure comparing with free OPH in solution due to its electrostatical binding to HOOC-FMS thereby displaying the increased fluorescence intensity. These results suggest the interactions of OPH with HOOC-FMS resulted in the protein immobilization and a favorable conformational change for OPH in the crowded confinement space and accordingly the enhanced activity.

Keywords

organophosphorus hydrolase; mesoporous silica; enzyme activity; conformational change; spectroscopic methods

Introduction

One of the key fundamental scientific questions is how isolated enzymes maintain their native active conformations in solution or in an immobilization matrix. Confinement theory and modeling efforts have predicted that 1) a protein or a protein-substrate complex inside a confined space would be stabilized by some folding forces not present for proteins in bulk

*Corresponding author: Dr. Chenghong Lei, Pacific Northwest National Laboratory, Mail Stop P7-56, P.O. Box 999, Richland, WA 99352, Tel: 1-509-3716962, Fax: 1-509-3717304, Chenghong.Lei@pnl.gov.

Publisher's Disclaimer: This is a PDF file of an unedited manuscript that has been accepted for publication. As a service to our customers we are providing this early version of the manuscript. The manuscript will undergo copyediting, typesetting, and review of the resulting proof before it is published in its final citable form. Please note that during the production process errors may be discovered which could affect the content, and all legal disclaimers that apply to the journal pertain.

NIH-PA Author Manuscript
NIH-PA Author Manuscript
NIH-PA Author Manuscript

NIH-PA Author Manuscript

NIH-PA Author Manuscript

NIH-PA Author Manuscript

solutions [1–3]; and 2) peptide chain unfolding, which could result in protein denaturation, would be less likely to occur inside the confined space because of excluded volume[3] [1–3]. In particular, when proteins are "confined" inside a biological living cell, they exhibit the highest activity, stability, and catalytic reaction rate.

Mesoporous silica has been extensively investigated for industrial and environmental processes because of its open pore structure, well-defined pore size and shape, and large surface area [4,5]. It can be synthesized with pore sizes from 20–500 Å (diameters) [5–7], a size range suitable for entrapping enzymes. With rigid, open pore structures and controllable pore sizes, mesoporous silica can facilitate mass transportation of the enzyme substrate and product. Both unfunctionalized and functionalized mesoporous silica have been tested for enzyme immobilization [8–16]. Our recent results have showed that the enzymes entrapped in functionalized mesoporous silica (FMS) with pore sizes as large as tens of nanometers could exhibit enhanced activity in comparison with the enzymes free in solution [17–21]. Among those findings, organophosphorus hydrolase (OPH) in HOOC-FMS displayed the specific activity nearly twice as much as that of OPH in solution, and the higher the loading density (P_{LD}) of OPH in FMS is, the higher specific activity it could display [17–20]. The preliminary analysis of the surface net charges of OPH demonstrated that, due to the prominent electrostatic interaction, the local region of OPH with the largest number of positive charges (+8.0) induces a favorable orientation of OPH in HOOC-FMS via attachment to negatively charged wall of HOOC-FMS, leaving the substrate entrance completely open even at a high P_{LD} [17].

In this work, to study the mechanisms of OPH activity enhancement in FMS, CD spectra and steady-state fluorescence are used to determine conformational change, solvent accessibility, protein dynamics, and structural stability of OPH in HOOC-FMS. We found that a favorable conformational change was resulted from the interaction of OPH with HOOC-FMS and thereby the OPH activity was enhanced.

Materials and methods

Materials

Organophosphorus hydrolase (OPH, dimer) was prepared as previously described [20], and the purified OPH was determined by SDS-polyacrylamide gel electrophoresis with Coomassie Blue staining corresponding to the expected monomer about 36 kDa. A stock solution of OPH (1.0 mg/mL) was prepared in 20–100 mM HEPES buffer (pH 7.2–7.5) and then stored at −80° C. The mesoporous silica (SBA-15) with 533 m^2/g surface area and 30 nm pore size, and the corresponding HOOC-FMS were prepared in a similar procedure as for the previous work [5,7,22]. A controlled hydration and condensation reaction was used to introduce functional groups into unfunctionalized mesoporous silica (UMS) [5,22]. The 2% HOOC-FMS is used throughout this work based on our previous results [17,19,20], where 2% of the total available surface area of UMS was silanized with trimethoxy silane with the functional group HOOC-. N-(2-hydroxyethyl)piperazine-N′-(2-ethanesulfonic acid) (HEPES), N-cyclohexyl-2-aminoethanesulfonic acid (CHES), and diethyl *p*-nitrophenyl phosphate, and paraoxon-ethyl were purchased from Sigma-Aldrich Chemical Co. (St. Louis, MO).

Assay of Enzyme Activity

OPH activity was measured in 1 mM of paraoxon in pH 9.0, 0.15 M CHES buffer at 25°C, in which one OPH unit is the active amount allowing 1.0 micromole paraoxon to be hydrolyzed per minute (Unit/mg OPH). OPH stock solution and OPH-FMS suspension were diluted 20–50 times by 20 mM HEPES (pH 7.5) for activity measurements. Multiple OPH stock solutions in different buffers were prepared with different initial specific activities. In this work, the

NIH-PA Author Manuscript

NIH-PA Author Manuscript

NIH-PA Author Manuscript

specific activities of OPH in solution were 900–1800 Units/mg in 20 mM HEPES (pH 7.5) and 500–700 Units/mg in 10 mM potassium phosphate (pH 7.5).

Preparation of Enzyme-FMS Composites

Typically, 0.2 mg OPH was used for incubation per mg of 2% HOOC-FMS, in which the enzyme was in excess. The incubation tubes were shaken at 1400 min^{-1} on an Eppendorf Thermomixer 5436 at room temperature (21 ± 1°C) for 2–3 h except the time-dependent experiments. Then OPH-FMS composite was centrifuged and washed in the working buffer. Finally, the washed deposit was resuspended in 100–300 μL of the working buffer per mg of original FMS for measurement. For the studies on the correlation of the enzyme specific activity with the protein loading density in FMS, limiting amounts of enzyme were incubated in aliquots of FMS to produce different protein loading densities (P_{LD}, μg OPH/mg of FMS). The protein concentration was measured using Bradford method (Bio-Rad) using bovine serum albumin as the protein standard.

Circular Dicroism (CD) Measurement of OPH and OPH Entrapped in FMS

CD were determined with Model 410 Circular Dichroism Spectrophotometer (Aviv Biomedical, Inc., Lakewood, NJ) with a path length of 1.0 cm. Measurements were carried out in 40 μg/mL of OPH in 10 mM potassium phosphate (pH 7.5). Two scans were accumulated and averaged for each spectrum after the background of blank buffers or HOOC-FMS was subtracted.

Steady-State Fluorescence Measurement

Fluorescence and anisotropy were measured with a Fluoro Max-2 fluorometer (SPEX, Edison, NJ), using excitation and emission slits of 5 nm. In all cases, control samples (blank buffers and HOOC-FMS in the absence of OPH) were used to determine the contribution of background fluorescence or scattered light to the observed spectra. Control samples demonstrated that these contribution were minimal (i.e., <5%). The solvent accessibility of fluorephores, tyrosinyl (Tyr) and tryptophanyl (Trp) residues of OPH was assessed through collisional quenching, where variable amounts of acrylamide were added to OPH solution (10 μg/mL). Data were analyzed as F_0/F as a function of the titrated acrylamide concentration according to the Stern-Volmer equation

$$F_0/F = 1 + K_{sv}[Q] \quad (1)$$

where F_0 and F are the respective fluorescence intensities in the absence and presence of acrylamide [Q], and K_{sv} is the Stern-Volmer quenching constant (*38, 39*).

Steady-state fluorescence anisotropy measurements were performed as described previously [23]. Single-point fluorescence anisotropy measurements were made at the maximum emission wavelength, using excitation at 295 nm for Trp residues of OPH. Steady-state fluorescence anisotropies (A) were calculated from the ratio of the fluorescence intensity (I) with the polarizers in vertical (v) or horizontal (h) position:

$$A = \frac{I_{vv} - gI_{vh}}{I_{vv} + 2gI_{vh}} \quad (2)$$

where $g = I_{hv}/I_{hh}$.

NIH-PA Author Manuscript

NIH-PA Author Manuscript

NIH-PA Author Manuscript

Results and Discussion

X-ray structure shows OPH consists of a distorted α/β barrel structure which is comprised of 2 parallel β-strands, 8 antiparallel β-strands and 14 α-helix [24–26]. CD is one of the most sensitive physical techniques for determining the secondary structure of polypeptides and proteins. We therefore first compare the CD spectra of OPH in HOOC-FMS with that of OPH free in solution. At pH 7.5, the overall positively-charged OPH (the isoelectric point of OPH is 8.3) could be spontaneously entrapped in HOOC-FMS due to electrostatic interaction [17, 19,20]. When OPH was incubated with HOOC-FMS, there was a rapid increase in protein loading density (P_{LD}, μg OPH/mg of FMS) within the first 2 hours, then reaching toward a stabilized loading density plateau. By controlling the amount of OPH incubated with HOOC-FMS, two OPH-FMS samples were prepared at P_{LD} of 30 and 49 μg/mg of FMS respectively. Fig. 1A shows that OPH specific activity was increased with increasing P_{LD} in HOOC-FMS in 10 mM potassium phosphate (pH 7.5) as expected [17]. Far-UV CD spectra were measured from 190 to 260 nm at 0.5 nm intervals for OPH and OPH-FMS in 10 mM potassium phosphate (pH 7.5), which are corresponding to electronic transitions of the backbone chromophore of the enzyme [27]. Fig. 1B shows the CD spectrum of OPH has strong double minima peaks at 222 nm and 209 nm, which are typical of α-helical content in the secondary structure of protein [27,28]. OPH-FMS displays a less negative peak at 222 nm and 209 nm, indicating that there was a secondary structural change when OPH was entrapped in HOOC-FMS. Table 1 shows the secondary structural fractions estimated from CD data using Aviv software. Upon entrapment of OPH in HOOC-FMS (P_{LD} = 30), the percentage of α-helix was decreased from 36.5 to 22.6%, while β-strand increased from 15.3 to 24.3%. There were also decreased α-helix, increased β-strand and disordered structure with increased loading density of OPH in HOOC-FMS (Table 1). The results demonstrate that HOOC-FMS induced α-helix/β-strand transition of OPH due to the electrostatic interaction of OPH with HOOC-FMS, and the favorable conformation of OPH therein contained more β-strand structure.

Fluorescence emission spectra were used to assess the microenvironmental changes of tyrosinyl (Tyr) and tryptophanyl (Trp) residues in OPH. Each subunit of OPH presents 8 significant emissive residues, four tyrosine (Tyr) and four tryptophanyl (Trp) residues [25, 29,30]. Trp 302, Trp 131 and Tyr 239 are located near the active site, and Trp 69 is located at the subunit interface [25,29,30]. The 278 nm was selected as the excitation wavelength for fluorescence spectroscopy, allowing excitation of both tyrosinyl and tryptophanyl residues in protein. Fig. 2A and 2B show that, in the absence of urea, the fluorescence emission spectrum of OPH in solution has an emission maximum near 334 nm after excitation at 278 nm at 25° C, indicating that fluorescence emission of OPH is predominantly contributed from Trp residues. There was a 42% increase in fluorescence intensity. Grimsley et al. reported that the fluorescence emission intensity of OPH decreased rapidly when the protein underwent from a folded state to an unfolded state with the increasing urea concentrations [28]. The earlier report has shown that OPH entrapped in HOOC-FMS displayed an increased K_{cat} (8.50×10^3 s^{-1}) in comparison with that of OPH free in solution ($K_{cat} = 5.35 \times 10^3$ s^{-1}) [17,19,20]. The increased fluorescence intensity of OPH demonstrate that there was a favorable conformational change upon OPH entrapment in HOOC-FMS because the OPH activity was significantly enhanced.

To address the chemical stability of OPH in HOOC-FMS, the conformational changes of OPH was further studied by measuring fluorescence spectra of its Trp residues in the presence of urea (Fig. 2). The denaturant-induced unfolding was observed for both OPH and OPH-FMS samples. OPH is a homodimer and the overall unfolding reaction would start with the folded homodimer and end with two unfolded monomers [28]. Fig. 2A and 2B show that, with increased concentrations of urea, the fluorescence intensity of OPH and OPH-FMS was significant decreased and the spectra were red-shifted. This was in agreement with the previously reported results, that is, the fluorescence intensity of OPH was decreased with

NIH-PA Author Manuscript

NIH-PA Author Manuscript

NIH-PA Author Manuscript

increasing urea concentrations accompanying the decreased OPH activity [28], vice versa. It was urea who induced OPH unfolding with more exposure of Trp residues to the solvent, accordingly the decreased fluorescence intensity. The urea-dependent structural transitions of OPH and OPH-FMS were compared with the changes in the fluorescence emission maximum (λ_{max}) (Fig. 3A). All data are fit using the Hill equation resolving the half-saturation urea concentrations ($K_{1/2}$) (Fig. 3A). The unfolding of OPH in solution induced by urea occurs at lower urea concentrations ($K_{1/2}$ = 3.7 M) in consistent with previously reported values, e.g., $K_{1/2}$ = 3.77 M [28]. In contrast, the half-saturation urea concentrations for OPH in HOOC-FMS was shifted to the higher urea concentrations ($K_{1/2}$ = 5.4 M). The increase of $K_{1/2}$ value indicates OPH entrapped in HOOC-FMS had a more stable conformational structure against urea-induced unfolding as compared to OPH free in solution.

Thermal denaturation experiments were performed by monitoring the steady-state fluorescence anisotropy for OPH as function of temperature. Fig. 3B shows, there is a decrease in the anisotropy for OPH in solution from 0.15 to 0.12 when incubating OPH solution between 20 and 65°C, indicating unfolding of the protein occurs. In contrast, entrapment of OPH in HOOC-FMS resulted in an increase in anisotropy from 0.15 to 0.18, that is, reduction of OPH domain motion (Fig. 3B). In addition, above 65°C, the anisotropy of Trp residues of OPH free in solution was increased rapidly, implying that OPH can be aggregated at the temperature over 65°C. However, there was a slower increase in the anisotropy for OPH-FMS at the temperature over 65°C, indicating that HOOC-FMS can maintain the thermal stability of the enzyme against the unfolding temperature comparing to that of the enzyme free in solution.

Possible causes underlying the observed differences in the intrinsic fluorescence intensity of OPH free in solution and entrapped in HOOC-FMS may be resulted from global changes in the tertiary structure of the enzyme that altered the microenvironment around the fluorophores. Therefore, the solvent accessibility of Trp residues was measured using acrylamide as a collisional quencher. The Stern-Volmer plot for OPH in solution is linear (Fig. 4), indicating a pure dynamic quenching of OPH by acrylamide. In the case of OPH entrapped in HOOC-FMS, there is a lower quenching constant (K_{sv} = 18.2 ± 0.8 M^{-1}) compared to that of OPH free in solution (K_{sv} = 20.5 ± 0.7 M^{-1}). This result indicates that there was a decrease in the solvent exposure of Trp residues upon OPH entrapment in HOOC-FMS. This has resulted in the increase of the fluorescence intensity of OPH upon entrapment in HOOC-FMS (Fig. 2), where the most positively-charged protein surface of OPH were electrostatically attached to HOOC-FMS [17], thereby the disassociation of protein domains was limited and the solvent accessibility of Trp residues of OPH could be restricted [17].

In summary, the conformation, solvent accessibility, protein dynamics of OPH entrapped in FMS were characterized by CD and fluorescence spectra. The molecular packing of OPH in HOOC-FMS via electrostatical interaction resulted in enhanced chemical and thermal stability of OPH comparing to OPH in solution. The CD and fluorescence spectra confirmed that there were some secondary and tertiary structural changes upon OPH entrapment in HOOC-FMS. Taking the enhanced activity and K_{cat} into account, we believe that FMS as a confined space provided an interactive nanoenvironment promoting a favorable protein conformational change, thereby enhancing enzyme activity and stability.

Acknowledgments

This work was supported by the NIH National Institute of General Medical Sciences (grant number R01GM080987). Pacific Northwest National Laboratory (PNNL) is operated for U.S. Department of Energy by Battelle under Contract DE-AC06-RLO1830. A portion of the research described in this paper was performed in the Environmental Molecular Sciences Laboratory, a national scientific user facility sponsored by the Department of Energy's Office of Biological and Environmental Research and located at PNNL.

NIH-PA Author Manuscript

NIH-PA Author Manuscript

NIH-PA Author Manuscript

References

1. Zhou HX. Protein folding and binding in confined spaces and in crowded solutions. Journal of Molecular Recognition 2004;17:368–375.
2. Zhou HX, Dill KA. Stabilization of proteins in confined spaces. Biochemistry 2001;40:11289–11293. [PubMed: 11560476]
3. Minton AP. The Influence of Macromolecular Crowding and Macromolecular Confinement on Biochemical Reactions in Physiological Media. J Biol Chem 2001;276:10577–10580. [PubMed: 11279227]
4. Bhatia RB, Brinker CJ. Aqueous sol-gel process for protein encapsulation. Chem Mater 2000;12:2434–2441.
5. Feng X, Fryxell GE, Wang LQ, Kim AY, Liu J, Kemner KM. Functionalized monolayers on ordered mesoporous supports. Science 1997;276:923–926.
6. Zhao D, Huo Q, Feng J, Chmelka BF, Stucky GD. Nonionic Triblock and Star Diblock Copolymer and Oligomeric Surfactant Syntheses of Highly Ordered, Hydrothermally Stable, Mesoporous Silica Structures. J Am Chem Soc 1998;120:6024–6036.
7. Zhao DY, Feng JL, Huo QS, Melosh N, Fredrickson GH, Chmelka BF, Stucky GD. Triblock copolymer syntheses of mesoporous silica with periodic 50 to 300 angstrom pores. Science 1998;279:548–552. [PubMed: 9438845]
8. Yiu HHP, Wright PA, Botting NP. Enzyme immobilisation using siliceous mesoporous molecular sieves. Microporous and Mesoporous Materials 2001;44–45:763–768.
9. Yiu HHP, Wright PA, Botting NP. Enzyme immobilization using SBA-15 mesoporous molecular sieves with functionalised surfaces. J Mol Catal B: Enzymatic 2001;15:81–92.
10. Han YJ, Watson JT, Stucky GD, Butler A. Catalytic activity of mesoporous silicate-immobilized chloroperoxidases. J Mol Catal B: Enzymatic 2002;17:1–8.
11. Han YJ, Stucky GD, Butler A. Mesoporous silicate sequestration and release of proteins. J Am Chem Soc 1999;121:9897–9898.
12. Takahashi H, Li B, Sasaki T, Miyazaki C, Kajino T, Inagaki S. Catalytic activity in organic solvents and stability of immobilized enzymes depend on the pore size and surface characteristics of mesoporous silica. Chem Mater 2000;12:3301–3305.
13. Washmon LL, Balkus KJ Jr. Cytochrome c immobilized into mesoporous molecular sieves. J Mol Catal B: Enzymatic 2000;10:453–469.
14. Gimon-Kinsel ME, Jimenez VL, Washmon LL, Balkus KJ Jr. Mesoporous molecular sieve immobilized enzymes. Stud Surf Sci Catal 1998;117:373–380.
15. Diaz JF, Balkus KJ Jr. Enzymes immobilized in MCM-41 molecular sieves. J Mol Catal B: Enzymatic 1996;2:115–126.
16. Deere J, Magner E, Wall JG, Hodnett BK. Mechanistic and structural features of protein adsorption onto mesoporous silicates. J Phy Chem B 2002;106:7340–7347.
17. Lei C, Soares TA, Shin Y, Liu J, Ackerman EJ. Enzyme Specific Activity in Functionalized Nanoporous Supports. Nanotechnology 2008;19:125102.
18. Lei C, Shin Y, Liu J, Ackerman EJ. Synergetic Effects of Nanoporous Support and Urea on Enzyme Activity. Nano Letters 2007;7:1050–1053. [PubMed: 17341123]
19. Lei C, Shin Y, Magnuson JK, Fryxell G, Lasure LL, Elliott DC, Liu J, Ackerman EJ. Characterization of Functionalized Nanoporous Supports for Protein Confinement. Nanotechnology 2006;17:5531–5538.
20. Lei C, Shin Y, Liu J, Ackerman EJ. Entrapping enzyme in a functionalized nanoporous support. J Am Chem Soc 2002;124:11242–11243. [PubMed: 12236718]
21. Dunker AK, Fernandez A. Engineering productive enzyme confinement. Trends in Biotechnology 2007;25:189–190. [PubMed: 17379337]
22. Liu J, Shin Y, Nie ZM, Chang JH, Wang LQ, Fryxell GE, Samuels WD, Exarhos GJ. Molecular assembly in ordered mesoporosity: A new class of highly functional nanoscale materials. J Phys Chem A 2000;104:8328–8339.

NIH-PA Author Manuscript

NIH-PA Author Manuscript

NIH-PA Author Manuscript

23. Chen BW, Lowry DF, Mayer MU, Squier TC. Helix A stabilization precedes amino-terminal lobe activation upon calcium binding to calmodulin. Biochemistry 2008;47:9220–9226. [PubMed: 18690719]
24. Benning MM, Shim H, Raushel FM, Holden HM. High Resolution X-ray Structures of Different Metal-Substituted Forms of Phosphotriesterase from Pseudomonas diminuta. Biochemistry 2001;40:2712–2722. [PubMed: 11258882]
25. Benning MM, Kuo JM, Raushel FM, Holden HM. 3-DIMENSIONAL STRUCTURE OF THE BINUCLEAR METAL CENTER OF PHOSPHOTRIESTERASE. Biochemistry 1995;34:7973–7978. [PubMed: 7794910]
26. Benning MM, Kuo JM, Raushel FM, Holden HM. 3-DIMENSIONAL STRUCTURE OF PHOSPHOTRIESTERASE - AN ENZYME CAPABLE OF DETOXIFYING ORGANOPHOSPHATE NERVE AGENTS. Biochemistry 1994;33:15001–15007. [PubMed: 7999757]
27. Zheng JY, Constantine CA, Rastogi VK, Cheng TC, DeFrank JJ, Leblanc RM. Secondary structure of organophosphorus hydrolase in solution and in Langmuir-Blodgett film studied by circular dichroism spectroscopy. Journal of Physical Chemistry B 2004;108:17238–17242.
28. Grimsley JK, Scholtz JM, Pace CN, Wild JR. Organophosphorus hydrolase is a remarkably stable enzyme that unfolds through a homodimeric intermediate. BIOCHEMISTRY 1997;36:14366–14374. [PubMed: 9398154]
29. Vanhooke JL, Benning MM, Raushel FM, Holden HM. Three-dimensional structure of the zinc-containing phosphotriesterase with the bound substrate analog diethyl 4-methylbenzylphosphonate. Biochemistry 1996;35:6020–6025. [PubMed: 8634243]
30. Zheng JY, Desbat B, Rastogi VK, Shah SS, DeFrank JJ, Leblanc RM. Organophosphorus hydrolase at the air-water interface: Secondary structure and interaction with paraoxon. Biomacromolecules 2006;7:2806–2810. [PubMed: 17025356]

NIH-PA Author Manuscript
NIH-PA Author Manuscript
NIH-PA Author Manuscript

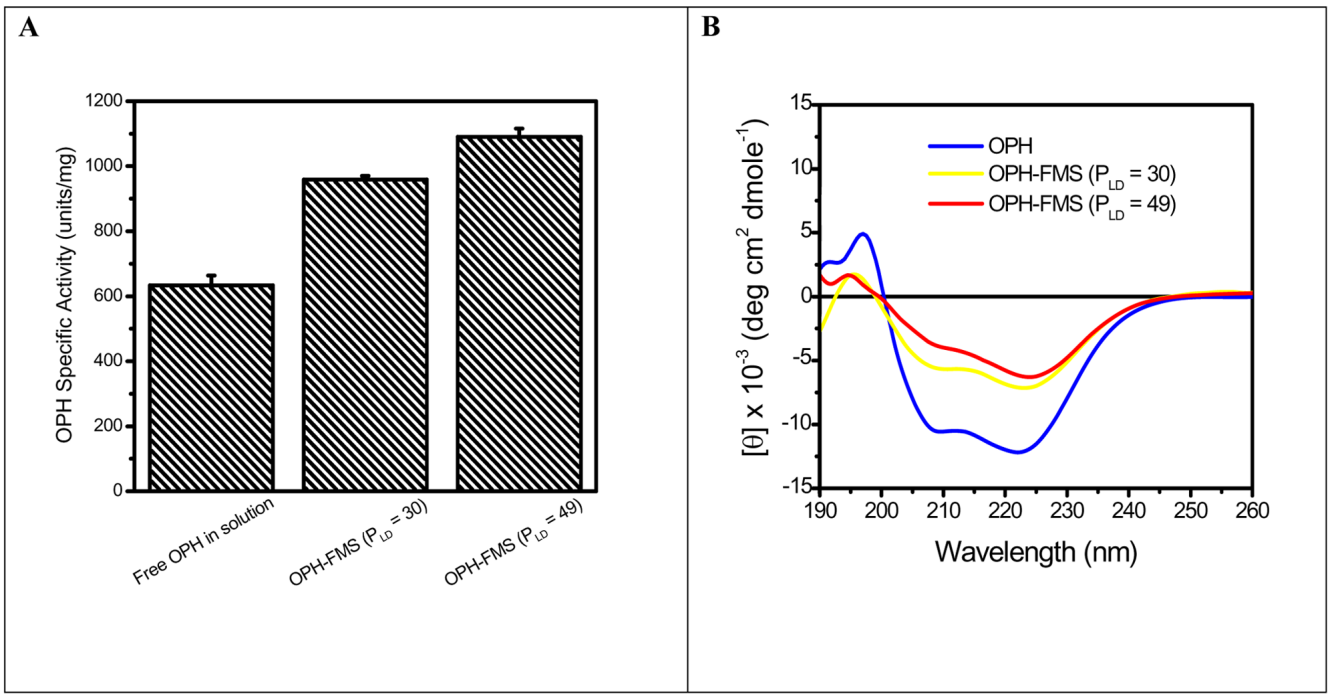

Fig. 1.

(A) Increased OPH specific activity with increasing P_{LD} of OPH in HOOC-FMS. The specific activity of OPH stock solution prior to the entrapping was 634 units/mg; **(B)** Circular dichroism spectra of OPH in solution and in HOOC-FMS. The measurements were carried out in 40 μg/mL of OPH. Working buffer: 10 mM potassium phosphate (pH 7.5) at 25°C.

NIH-PA Author Manuscript
NIH-PA Author Manuscript
NIH-PA Author Manuscript

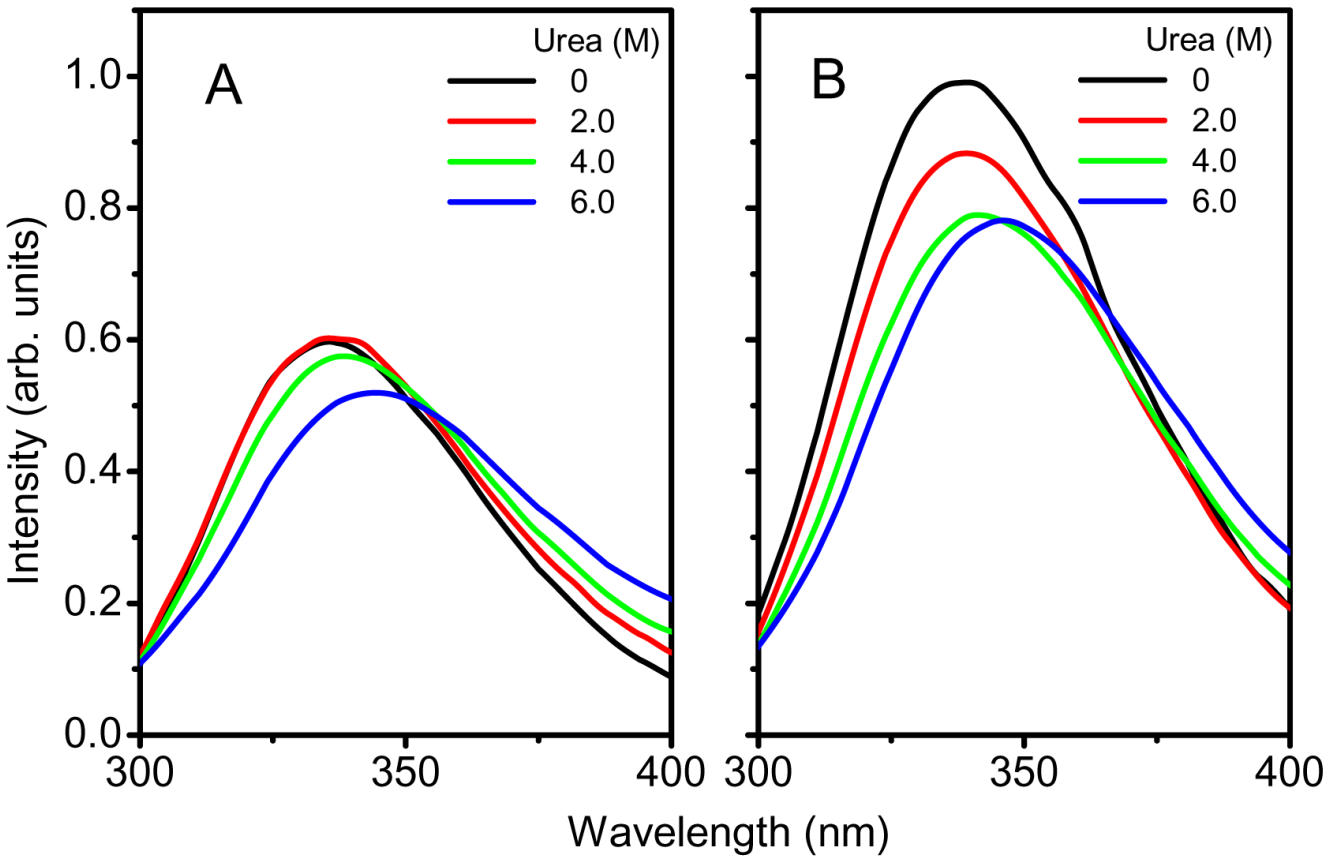

Fig. 2.

Changes in fluorescence spectra of Tyr and Trp residues of OPH in solution (**A**) and OPH in HOOC-FMS (**B**) (P_{LD} = 53) during chemical denaturation using urea at different concentrations. The samples contained 10 μg/mL of OPH in 20 mM HEPES (pH 7.5). The specific activity of OPH in solution was 1690 units/mg, while the specific activity of the resulted OPH-FMS was 2569 units/mg. The fluorescence emission was measured with excitation at 278 nm at 25°C.

NIH-PA Author Manuscript
NIH-PA Author Manuscript
NIH-PA Author Manuscript

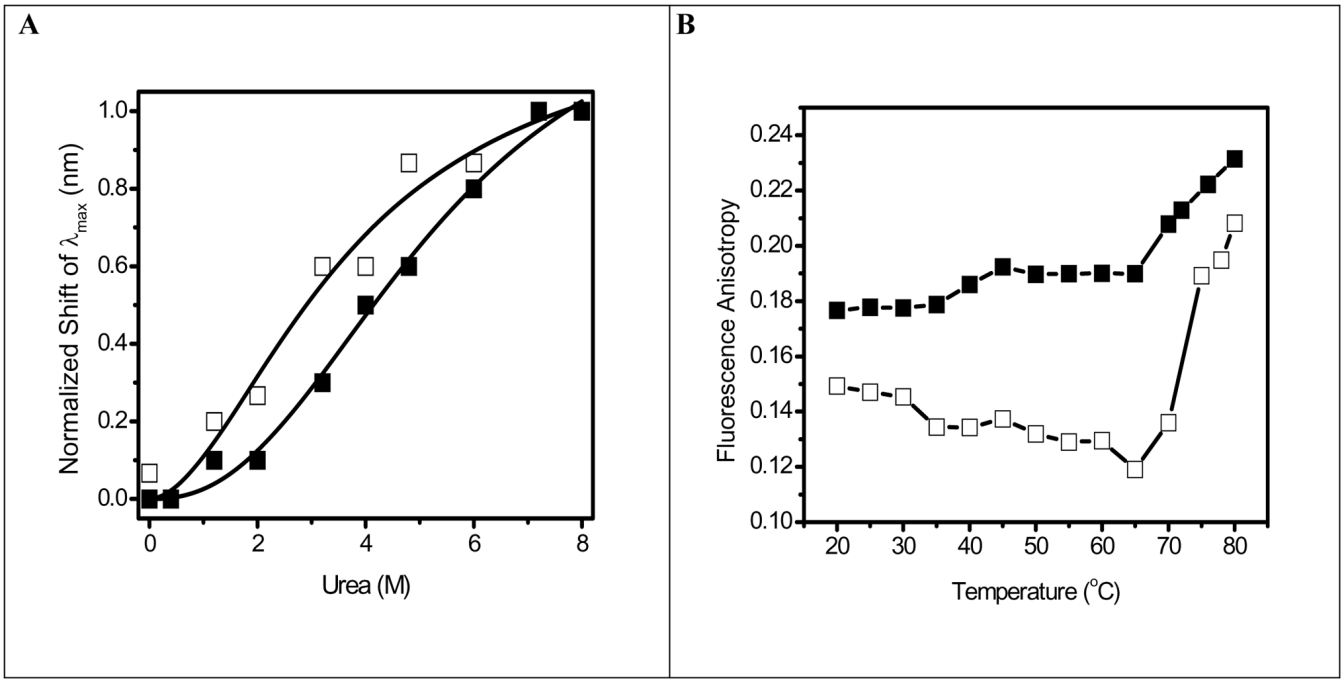

Fig. 3.

Fig. 3A. Shift in fluorescence emission maximum for OPH in solution (□)and OPH in HOOC-FMS (P_{LD} = 53) (■) during chemical unfolding using urea. The samples contained 10 μg/mL of OPH in 20 mM HEPES (pH 7.5). The specific activity of OPH in solution was 1690 units/mg, while the specific activity of the resulted OPH-FMS was 2569 units/mg. Line represents a nonlinear least squares fit to changes in fluorescence wavelength λ_{max}) to the Hill equation $Y=[\text{Urea}]^n/(K^n_{1/2}+[\text{Urea}]^n)$, where n is the Hill coefficient (~2) and $K_{1/2}$ is the half-saturation urea concentration. The obtained $K_{1/2}$ is 3.7 M for OPH in solution, 5.4 M for OPH in HOOC-FMS.

Fig. 3B. Temperature-dependent changes in fluorescence anisotropy of Trp for OPH in solution (□) and OPH in HOOC-FMS (P_{LD} = 62 μg/mg) (■). The samples contained 50 μg/mL of OPH in 10 mM potassium phosphate (pH 7.5) at 25°C. The specific activity of OPH in solution was 915 units/mg, while the specific activity of the resulted OPH-FMS was 1598 units/mg. Steady-state fluorescence anisotropy was measured at 334 nm with excitation at 295 nm at 25°C.

NIH-PA Author Manuscript
NIH-PA Author Manuscript
NIH-PA Author Manuscript

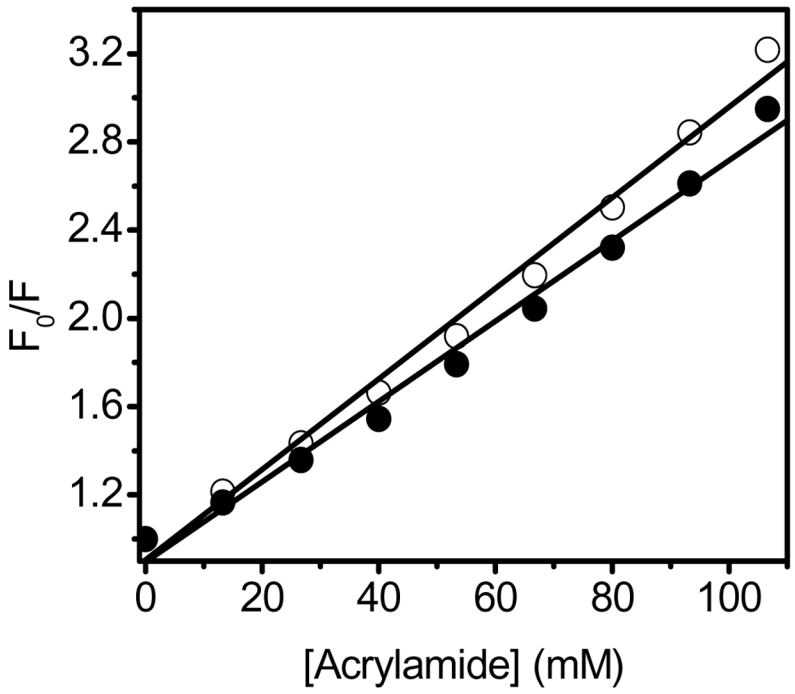

Fig. 4.

The Stern-Volmer plots of OPH (○) and OPH-FMS (●). F_0 and F are the respective fluorescence intensities in the absence and presence of acrylamide (see *Materials and Methods*) The emission fluorescence intensity of Trp residues at 334 nm was measured using acrylamide as a collisional quencher with excitation at 278 nm at 25°C. The slopes of the lines were defined as the Stern-Volmer quenching constant, K_{sv}. The samples contained 10 μg/mL of OPH in 20 mM HEPES (pH 7.5). The specific activity of OPH in solution was 1690 units/mg, while the specific activity of the resulted OPH-FMS was 2569 units/mg.

NIH-PA Author Manuscript

NIH-PA Author Manuscript

NIH-PA Author Manuscript

Table 1

Secondary Structure Fraction of OPH in Solution and in HOOC-FMS*

	Percentage of Secondary Structure			
	α-Helix	**β-Sheet**	**β-Turn**	**Random Coil**
OPH	36.5	15.3	16.1	31.2
OPH-FMS ($P_{LD;}$ μg/mg)				
30	22.6	24.3	18.7	43.0
50	19.3	27.2	19.4	46.2

*Secondary Structure Fractions were estimated using Aviv CD Software.